Hypoxia-induced Circular RNA hsa_circ_0006508 Promotes the Warburg Effect in Colorectal Cancer Cells

Yugang Xu[1], Ying Zhang[2], Wenli Hao[1], Wen Zhao[3], Guang Yang[1], Changqing Jing[4]

[1]Department of General Surgery, The Affiliated Taian City Central Hospital of Qingdao University, Qingdao, China
[2]Department of Hepatobiliary Surgery, The Affiliated Taian City Central Hospital of Qingdao University, Taian, China
[3]Department of General Surgery, The Second People's Hospital of Daiyue District, Taian, China
[4]Department of General Surgery, Shandong Provincial Hospital, Shandong, China

Background: The hypoxia-induced Warburg effect promotes colorectal cancer malignancy with altered circular RNA (circRNA) expression.

Aims: To investigate the association with the Warburg effect in colorectal cancer and whether has_circ_0006508 can be induced by hypoxia.

Study design: In vitro cell lines and human-sample study.

Methods: The biological functions of circ_0006508 and miR-1272 in the viability, colony formation, and glycolysis under hypoxic conditions were determined by loss-of-function and gain-of-function experiments. The chromatin immunoprecipitation assay was used to demonstrate the direct binding between circ_0006508 promoters and hypoxia-inducible factor 1α (HIF-1α). Transcription activity was subjected to the Luciferase reporter assay. The correlation of circ_0006508 and miR-1272 with overall survival was determined with the Kaplan-Meier analysis.

Results: Upregulated circ_0006508 and downregulated miR-1272 were observed in colorectal cancer samples, which was associated with the TNM stage and overall survival. Functional assays demonstrated that the hypoxia-induced upregulated circ_0006508 and downregulated miR-1272 promoted the viability and Warburg effect of colorectal cancer in vitro. Mechanistically, HIF-1α-induced circ_0006508 could directly sponge miR-1272, which played a suppressive role in glycolysis.

Conclusion: Circ_0006508-mediated miR-1272 inhibition could promote the malignant behaviors of colorectal cancer with an upregulated Warburg effect.

INTRODUCTION

Approximately 20% of patients with colorectal cancer (CRC) have metastatic disease at presentation, and fewer than 20% of the patients survive beyond 5 years from the diagnosis.[1,2] Conventional systemic cytotoxic chemotherapy, biologic therapy, immunotherapy, and their combination can only offer palliative relief without decisive progress in overall survival (OS).[3,4]

The relapse and chemotherapy resistance of CRC can be attributed to the diversity of CRC metabolic reprogramming.[5-7] The Warburg effect, as a part of metabolic reprogramming, describes the hallmark that tumor cells preferentially utilize glycolysis to gain energy rather than oxidative phosphorylation in the hypoxic microenvironment, even in the presence of oxygen. Hypoxia-inducible factor 1 (HIF-1) reprograms high levels of glucose uptake and promotes pyruvate oxidation to lactic acid conversion, which stimulates rapid tumor proliferation.[8-10] These indicate the essence of investigating the potential mechanism leading to metabolic reprogramming.

Circular RNAs (circRNAs), as single-stranded non-coding RNA molecules, can function in RNA alternative splicing, miRNA sponges, and *in cis* transcription regulation to modulate metabolic reprogramming.[11-14] CircDENND4C, which is upregulated by HIF-1α in a hypoxic environment, can aggressively promote the proliferation of breast cancer cells with enhanced Warburg effect.[15]

CircFOXP1 is reported to promote gallbladder progression with the upregulated pyruvate kinase L/R expression and increased the Warburg effect.[16]

A previous study demonstrated that hsa_circ_0006508, which is derived from the host gene of vacuole membrane protein 1 (*VMP1*), was increased in CRC tissues.[17] However, investigations about its function in CRC are scarce. Thus, in this study, whether hsa_circ_0006508 can be induced by hypoxia and its association with the Warburg effect in CRC are investigated.

MATERIALS AND METHODS

Tissue Samples

Seventy CRC specimens and paired adjacent samples were collected from patients with CRC during surgery at Taian City Central Hospital, which were snap-frozen in liquid nitrogen. The relevant TNM stage classification and OS data were retrieved.

The Ethics Committee of Taian City Central Hospital approved the whole-sample retrieval and data-collection processes, and all patients provided written informed consent.

CRC Cell Culture

HCT-116 and HT-29 cells (American Type Culture Collection, Manassas, VA, USA) were cultured in a normoxic incubator (37 °C, 5% CO_2; Thermo Fisher, Waltham, MA, USA) or cultured in a hypoxia incubator chamber (5% CO_2, 1% O_2, and 94% N_2; StemCell, Hangzhou, China) in McCoy's 5A medium supplemented with fetal bovine serum (10%, Hyclone, Logan, UT, USA).

Transfection

HIF-1α siRNA 1 (si-HIF-1α-1, CUGAUGACCAGCAACUUGA), HIF-1α siRNA 2 (si-HIF-1α-2, CUGAUGACCAGCAACUUGA), circ_0006508-1-siRNA (si-circ_0006508-1, GTAGCAATGA ACAAGGAACAT), circ_0006508-2-siRNA (si-circ_6508-2, GGAAATCCTTGTAATCTTGAA), miR-1272 mimics, and control mimics were obtained from GeneChem (Shanghai, China), which were further transfected to 50 nM using Lipofectamine 3000 (Invitrogen). Total RNA was extracted 48 h post-transfection to confirm the transfection effects.

Cell Viability Detection

HT-29 and HCT-116 cells were plated in 96-well microplates ($5x10^3$ cells/well) for 48 h. Then, the cells were assayed with CCK-8 reagents (Dojindo Molecular Technologies, Kumamoto, Japan) at 37 °C for 1 h according to the manufacturer's recommendation. The absorbance value was detected by a microplate reader at 450 nm.

Colony Formation

HT-29 and HCT-116 cells were maintained for 2 weeks in six-well plates ($1x10^3$ cells/well). Then, the colonies were fixed with paraformaldehyde (4%) and subjected to crystal violet staining. The numbers were further counted.

Glucose Uptake

For glucose uptake analysis, the fluorescent glucose analog (100 μmol/l, K682-50, Biovision, Milpitas, CA, USA) contained in phosphate-buffered solution was used to incubate the cells for 1 h. The incubated cells were further lysed with trypsin-ethylenediaminetetraacetic acid (0.25%, Solarbio, Beijing, China) and stained with propidium iodide (5 mg/ml) at room temperature for 5 min. The relative fluorescence units (RFU%) were detected with flow cytometry.

Lactate and Pyruvate Production

Lactic acid and pyruvate quantification in supernatants was conducted using L-lactate and pyruvate assay kits (Abcam, Cambridge, MA, USA), respectively, according to the manufacturer's recommendation. The levels of lactic acid and pyruvate were assayed with spectrophotometer (Thermo Fisher) at 450 nm or 570 nm.

Cytosolic/Nuclear Fractionation

A hypotonic buffer was used to pre-incubate cells on ice for 5 min, and a hypotonic buffer supplemented with 1% NP-40 was added and incubated for another 5 min, which was centrifuged (5000 g, 5 min) to get the supernatant as the cytosolic fraction. Nuclear resuspension buffer was utilized to resuspend the pellets, which was further centrifuged (12000 g, 10 min) to get the supernatant as the nuclear fraction. U6 served as the control.

Quantitative Reverse-transcription Polymerase Chain Reaction

Total RNA was extracted with RNAiso Plus (Takara), which were further reverse-transcribed using the PrimeScript RT Master Mix and One Step PrimeScript miRNA cDNA Synthesis Kit (Takara).

The amplification was detected with SYBR Green master mix (Roche). The primer sequences were as follows: circ_0006508, forward: 5'-AGTGAATGAAAAGAAGAGGA-3', reverse: 5'-CAGATAAAGCAGAAAGGTGT-3'; miR-1272, forward: 5'- GCTGATGATGATGGCAGCAAA-3', reverse: 5'- GAGGTATTCGCACCAGAGGA-3'; *β-actin*, forward: 5'-GGCTGTGCTATCCCTGTACG-3', reverse: 5'-CTTGATCTTCATTGTGCTGGGTG-3'; U6, forward: 5'- GCTCGCTTCGGCAGCACA-3', reverse: 5'-GAGGTATTCGCACCAGAGGA-3'. The mRNA expression was normalized to *β-actin* or U6 levels and quantified using the $2^{-\Delta\Delta CT}$ method.

Western Blot

The cell lysate was separated with sodium dodecyl-sulfate polyacrylamide gel electrophoresis, which was further transferred to polyvinylidene fluoride membrane. The membrane was incubated with HIF-1α antibody (1:1000, Abcam) at 4 °C overnight. A secondary antibody was used for membranes incubated at room temperature for 2 h. The relative intensity of interest band was developed with an ECL system (GE Healthcare, Chicago, IL, USA) and calculated by correcting with β-actin.

Luciferase Assay

HT-29 and HCT-116 cells were transfected with miR-1272 mimics and luciferase reporter containing wild-type circ_0006508 promoter (forward, 5'-CCTTCTCGAGCTCCTCAAGAGTTACTGA-3'; reverse, 5'-CCTTGCGGCCGCCAGATAAAGCAGAAAGGTGT-3', circ_0006508-wide) or mutated-type circ_0006508 promoter (forward, 5'- GCAATGAACAAGGAAGCTGACAA-3'; reverse, 5'-TTGTCAGCTTCCTTGTTCATTGC-3', circ_0006508-mut) in 24-well plates for 48 h. The relative luciferase activity was further determined after cell lysis.

Chromatin Immunoprecipitation (ChIP) Assays

EpiQuiktm Chromatin Immunoprecipitation Kit and anti-HIF-1α (Abcam) antibody were used following the manufacturer's protocols. Polymerase chain reactions amplified the bound DNA sequences, which were separated by agarose gel electrophoresis. The corresponding immunoglobulin G was applied as the control.

Statistics

Data were expressed as the mean ± standard deviation (SD). Statistical analyses were conducted using GraphPad software. One-way analysis of variance (ANOVA), Student's t-test, or two-way ANOVA was utilized for data analysis. Statistical significance was determined when the p-value was <0.05.

RESULTS

HIF-1α Mediated circ_0006508 up-regulation in CRC Cells

HIF-1α was induced in HT-29 and HCT-116 cells under hypoxic condition after 24 and 48 h of culture compared with normoxic conditions (Figure 1a), and the corresponding upregulated circ_0006508 expressions were observed (Figure 1b). Additionally, si-HIF-1α-transfected HT-29 and HCT-116 cells were successfully constructed and confirmed by the diminished HIF-1α expression (Figure 1c), and further analysis indicated that specific siRNAs against HIF-1α could diminish the relative expression of circ_0006508 (Figure 1d). Hypoxia could induce the upregulated luciferase activity of circ_0006508 promoters in HCT-116 and HT-29 cells (Figure 1e, 1f), which could be inhibited by si-HIF-1α treatment in HCT-116 (Figure 1g) and HT-29 (Figure 1h) cells. The ChIP assay demonstrated that circ_0006508 promoters could be enriched on HIF-1α upon induced hypoxia (Figure 1ı and 1j). These data suggest that HIF-1α could bind directly to circ_0006508 promoters and promote the transcription activity of circ_0006508 upon hypoxia induction.
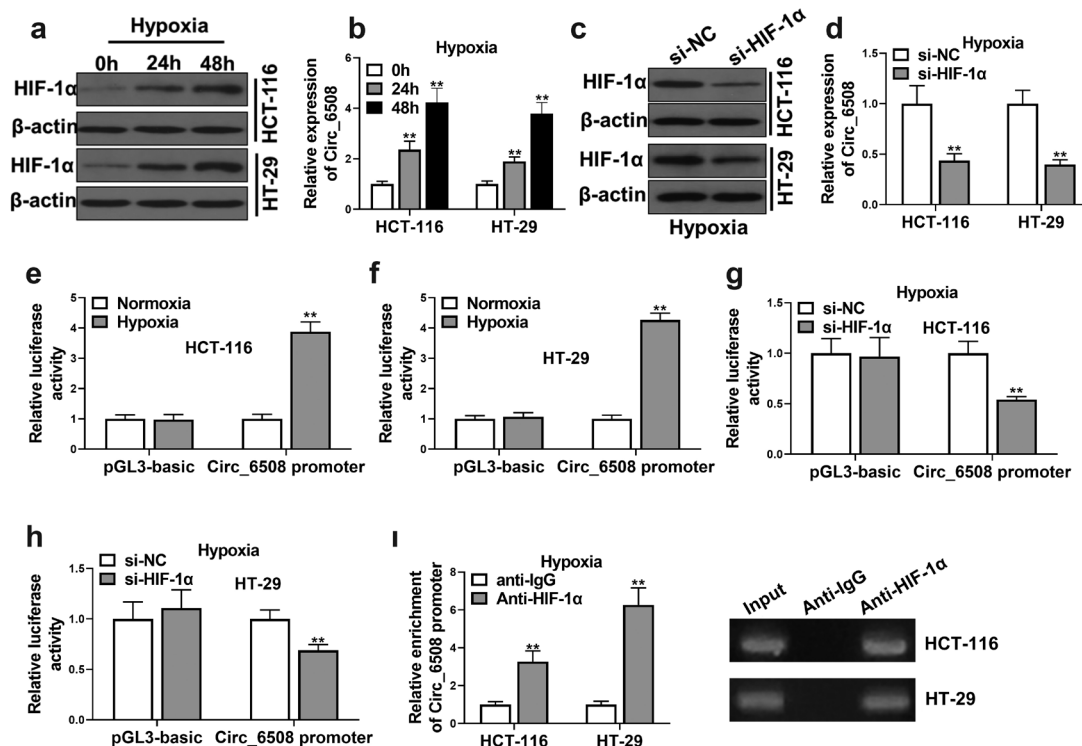

FIG. 1. Circ_0006508 was induced by hypoxia in CRC cells. HIF-1α was assayed with Western blot under hypoxic conditions for 0 h, 24 h, and 48 h (a). Circ_0006508 expression detected by qRT-PCR under hypoxic conditions for 0 h, 24 h, and 48 h (b). HIF-1α levels in both HT-29 and HCT-116 cells transfected with si-HIF-1α or negative control siRNAs (si-NC) under hypoxia for 48 h (c). Circ_0006508 expression detected by qRT-PCR in HT-29 and HCT-116 cells transfected with si-HIF-1α or si-NC under hypoxia for 48 h (d). Luciferase reporter assays in HCT-116 (e) and HT-29 (f) cells transfected with circ_0006508 promoter under normoxia or hypoxia for 48 h. Luciferase reporter assays in both HCT-116 (g) and HT-29 (h) cells with circ_0006508 promoter and si-HIF-1α co-transfection under hypoxia for 48 h. The direct binding between circ_0006508 promoters and HIF-1α was quantified (ı) and assayed (j) with ChIP. Data are presented as mean ± SD from three independent experiments. *$p < 0.05$; **$p < 0.01$.

Circ_0006508 Knockdown Inhibits the Proliferation and Glycolysis of CRC Cells Under Hypoxia

The knockdown efficiency of circ_0006508 was proven by the downregulated circ_0006508 expressions in HT-29 and HCT-116 cells (Figure 2a). Circ_0006508 knockdown could significantly inhibit the proliferation of HCT-116 and HT-29 cells (Figure 2b, 2c) and the in vitro colony formation ability (Figure 2d, $p <$ 0.01). Moreover, circ_0006508 knockdown significantly inhibited glucose uptake (Figure 2e), pyruvate production (Figure 2f), and lactate production (Figure 2g) in CRC.

Circ_0006508 Sponges miR-1272 in CRC Cells

The localization of circular RNA in cells determines its mode of action, and most of the circRNAs in the cytoplasm can act as ceRNAs. Initially, we detected the distribution of circ_0006508 in cells, which was revealed by circ_0006508 detection after nucleocytoplasmic separation, and circ_0006508 was mainly located in the cytoplasm of HCT-116 and HT-29 cells (Figure 3a, 3b). Mutant luciferase reporter vectors of circ_0006508

(Figure 3c) were constructed based on the predicted binding sites of circ_0006508 with miR-1272 derived from the circRNA interactome database. circ_0006508 was found to interact with miR-1272 with the downregulated luciferase intensities, whereas mutant circ_0006508 did not show the downregulated miR-1272 luciferase activities in HCT-116 and HT-29 cells (Figure 3d and 3e). In addition, we found that circ_0006508 knockdown could lead to the significantly upregulated miR-1272 expression (Figure 3f). These results prove the validity of circ_0006508 sponging on miR-1272 to downregulate the relative expression in CRC cells.

MiR-1272 Plays a Suppressive Role in CRC Glycolysis

Constructed miR-1272-overexpressed HCT116 and HT29 cells (Figure 4a) were utilized to decipher the role of miR-1272 in CRC cells. miR-1272 overexpression could significantly inhibit CRC cell viability (Figure 4b, 4c) and colony formation (Figure 4d) in vitro. Moreover, miR-1272 overexpression significantly inhibited the glucose uptake (Figure 4e), pyruvate production (Figure 4f), and lactate production (Figure 4g) of CRC. Therefore, miR-1272 overexpression could prohibit cell proliferation and glycolysis.
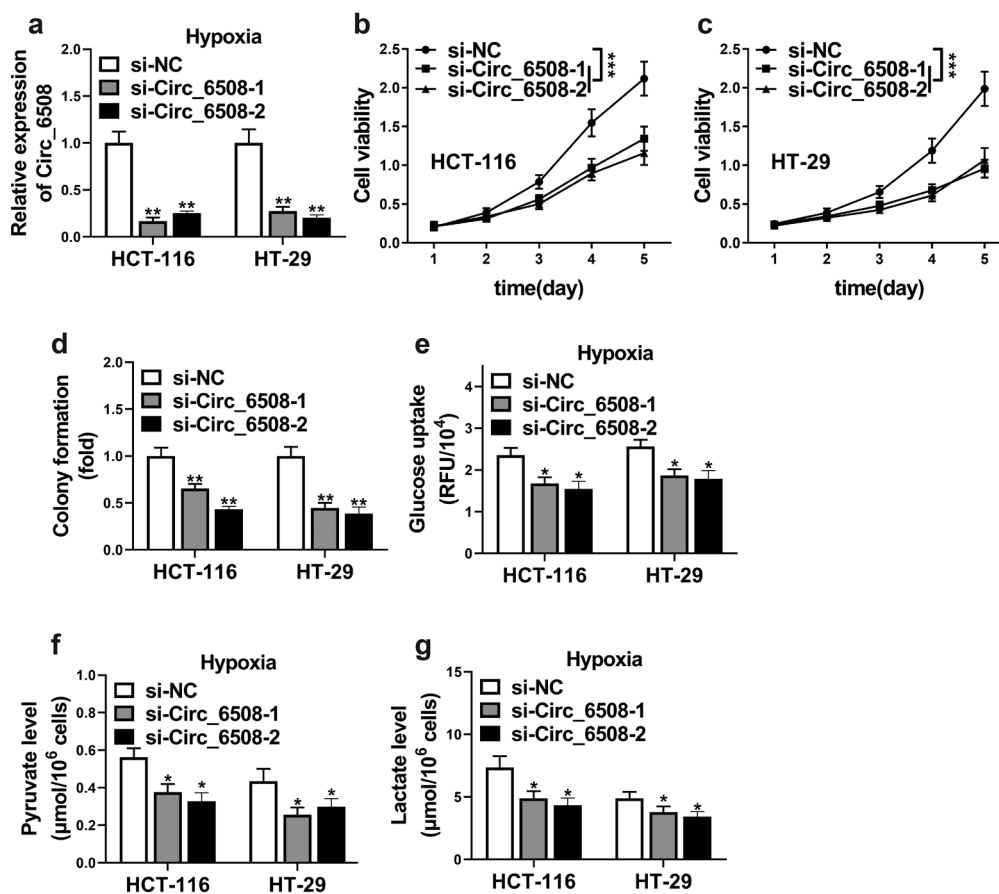

FIG. 2. Circ_0006508 depletion suppressed the proliferation and glycolysis of CRC cells under hypoxia. Knockdown efficiency of si-circ_0006508 in HT-29 and HCT-116 cells under hypoxia for 48 h (a). Effect of si-circ_0006508 on the viability of HCT-116 (b) and HT-29 cells (c), and colony formation (d) under hypoxia for 48 h. Glucose uptake (e), pyruvate production (f), and lactate production (g) were measured using commercially available kits. Data are presented as the mean ± SD from three independent experiments. $*p < 0.05$; $**p < 0.01$; $***p < 0.001$.
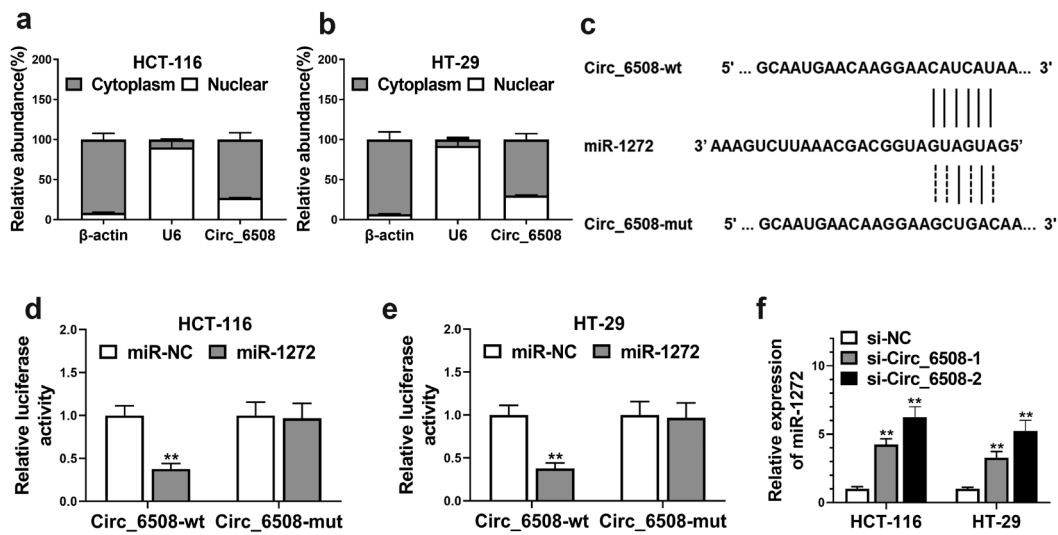
FIG. 3. Circ_0006508 targeted miR-1272 in CRC cells. Circ_0006508 expression was assayed with qRT-PCR in different subcellular fractionations of HCT-116 (a) and HT-29 (b) cells. The binding sequences of circ_0006508 in miR-1272 were predicted using the circRNA interactome database (c). Luciferase intensities of the wild-type and mutant luciferase reporter vectors of circ_0006508 in HCT-116 (d) and HT-29 (e) cells transfected with miR-1272. Expressions of miR-1272 in si-circ_0006508-transfected HT-29 and HCT-116 cells (f). Data are presented as the mean ± SD from three independent experiments. *$p < 0.05$; **$p < 0.01$.
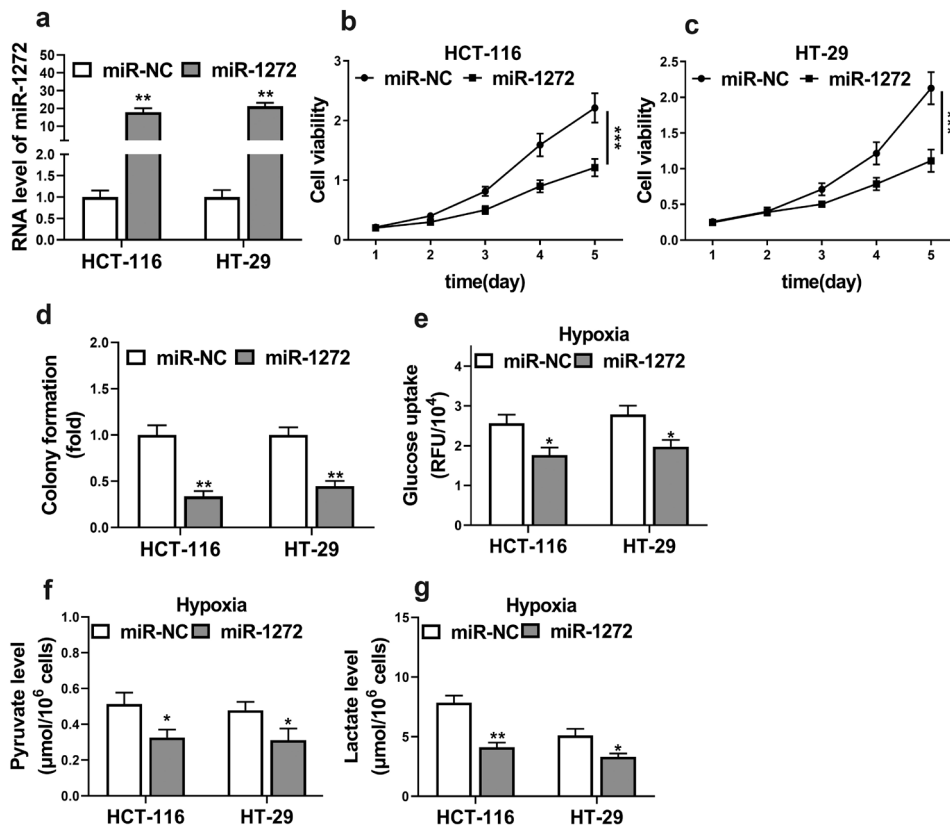

FIG. 4. MiR-1272 played a suppressive role in CRC glycolysis. (aa) MiR-1272 expression in HT-29 and HCT-116 cells transfected with miR-1272 mimics. The cell viability of HCT-116 (b) and HT-29 cells (c) transfected with miR-1272 mimics. The colony formation was also performed (d). Glucose uptake (e), pyruvate production (f), and lactate production (g) were measured in miR-1272 mimics transfected HCT-116 and HT-29 cells under hypoxia for 48 h using commercially available kits. The data represented the mean ± SD from three independent experiments. *$p < 0.05$; **$p < 0.01$; ***$p < 0.001$.

Circ_0006508 and miR-1272 Expression Correlates with CRC Malignancy

No significant differences in age, sex, tumor size, and differentiation status were observed in patients with low or high circ_0006508 expressions, whereas a significant difference was found in the TNM staging and lymph node status (Table 1).

Significantly increased circ_0006508 expression was assayed in 70 paired CRC tissues and compared with noncancerous tissues (Figure 5a, $p = 0.0067$), which positively correlated with the TNM stage as indicated by the high circ_0006508 expression in stages IV and III compared with stages II and I (Figure 5b, $p = 0.0005$). In comparison, the relative miR-1272 expression was dramatically suppressed in CRC tissues (Figure 5c, $p = 0.0011$), which negatively correlated with the TNM stage as indicated by the downregulated expression in stages IV and III compared with stages II and I (Figure 5d, $p = 0.0023$). The Kaplan–Meier analysis showed that higher circ_0006508 (Figure 5e, $p = 0.0136$) and lower miR-1272 (Figure 5f, $p = 0.0081$) could predict the worse survival rate of patients with CRC. These results demonstrate that altered circ_0006508 and miR-1272 expressions correlate with CRC malignancy characterized by the TNM stage and OS stratification.

DISCUSSION

In this study, upregulated circ_0006508 expression and downregulated miR-1272 expression were identified in human CRC samples, which correlated with the malignancy according to the TNM stage and OS analysis. Mechanically, circ_0006508 can sponge miR-1272 to induce increased proliferation, colony

formation, and Warburg effect, which are promoted by induced hypoxia. Hypoxia-induced HIF-1α could bind directly and promote the transcription activity of circ_0006508 to modulate metabolic reprogramming.

VMP1, the host gene of circ_0006508, has an essential role in balancing autophagy and apoptosis, contributing to the tumor metastasis process.[18] Epithelial cancer cells promote the Warburg effect in neighboring autophagy-activated stromal fibroblasts to facilitate tumor development.[19] In CRC, *VMP1*-mediated autophagy is proven to be pro-survival.[20] circRNA production was generally believed to compete with canonical pre-mRNA splicing to reduce host gene mRNA expression.[21,22] Whether circ_0006508 could decrease the host gene of *VMP1* and the relevant autophagy process to promote the Warburg effect requires further detailed analysis.

At present, only a few studies have attempted to decipher the functions of miR-1272. miR-1272 could revert the mesenchymal phenotype by interfering with the growth, migration, and invasion of prostate cancer through the inhibition of huntingtin-interacting protein 1.[23] miR-1272 was also reported to suppress the proliferation

TABLE 1. Demographic and Clinical Characteristics of Patients with colorectal cancer.

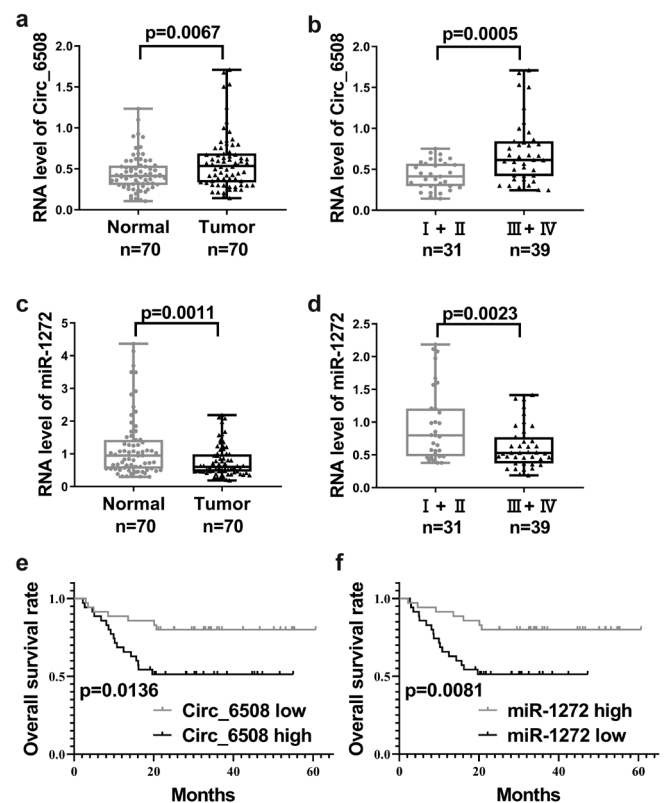| Variables	Expression of circ_0006508		
	Low (%)	High (%)	*P* value
Age			0.3388
<50	16 (44.44%)	20 (55.56%)	
≥50	19 (55.88%)	15 (44.12%)	
Sex			0.3340
Male	18 (45.00%)	22 (55.00%)	
female	17 (56.67%)	13 (43.33%)	
TNM staging			0.0303
I-II	20 (64.52%)	11 (35.48%)	
III-IV	15 (38.46%)	24 (61.54%)	
Tumor size (cm)			0.0921
<5	19 (61.29%)	12 (38.71%)	
≥5	16 (41.03%)	23 (58.97%)	
Differentiation			0.0557
Low	13 (38.24%)	21 (61.76%)	
Moderate and high	22 (61.11%)	14 (38.89%)	
Lymph node status			0.0271
Positive	9 (33.33%)	18 (66.67%)	
Negative	26 (60.47%)	17 (39.53%)	

FIG. 5. Circ_0006508 and miR-1272 were dysregulated in CRC. (a) Circ_0006508 expression in paired CRC tissues (*n* = 70). (b) Circ_0006508 expressed in CRC tissues based on the TNM stage. (c) miR-1272 expression in 70 paired CRC tissues and noncancerous tissues. (d) MiR-1272 expression in CRC tissues based on the TNM stage. Overall survival analysis with Kaplan–Meier based on the expressions of circ_0006508 (e) and miR-1272 (f).

and migration of glioma *via* the CDCP1 pathway.[24] In this study, miR-1272 inhibited the viability and glycolysis of CRC cells in vitro*,* which could be regulated by circ_0006508. Our findings will lay down a foundation for miR-1272 research in the future study of cancer treatment.

This study has some limitations. First, the precise mechanism of miR-1272-mediated glycolysis is not deciphered in this study. Second, there is also no relevant research on this topic; thus, further investigations are warranted. Third, the HIF-1α-dependent *VMP1*-mediated autophagic pathway was reported to induce resistance to photodynamic therapy in CRC.[25] Thus, whether such a mechanism is also involved in HIF-1α-induced *VMP1* expression needs further detailed analysis. Moreover, the function of circ_0006508 should be further verified in animal models.

Circ_0006508-mediated miR-1272 inhibition could promote the malignant tumor behaviors in CRC with upregulated Warburg effect. Our findings reveal that circ_0006508 and miR-1272 may be therapeutic targets for CRC treatment.

REFERENCES

1. Biller LH, Schrag D. Diagnosis and Treatment of Metastatic Colorectal Cancer: A Review. *JAMA.* 2021;325:669-685. **[CrossRef]**
2. Akimoto N, Ugai T, Zhong R, et al. Rising incidence of early-onset colorectal cancer - a call to action. *Nat Rev Clin Oncol.* 2021;18:230-243. **[CrossRef]**
3. Hull MA, Rees CJ, Sharp L, Koo S. A risk-stratified approach to colorectal cancer prevention and diagnosis. *Nat Rev Gastroenterol Hepatol.* 2020;17:773-780. **[CrossRef]**
4. Jung G, Hernández-Illán E, Moreira L, Balaguer F, Goel A. Epigenetics of colorectal cancer: biomarker and therapeutic potential. *Nat Rev Gastroenterol Hepatol.* 2020;17:111-130. **[CrossRef]**
5. Kitazawa M, Hatta T, Sasaki Y, et al. Promotion of the Warburg effect is associated with poor benefit from adjuvant chemotherapy in colorectal cancer. *Cancer Sci.* 2020;111:658-666. **[CrossRef]**
6. Song K, Guo Y, Wang X, et al. Transcriptional signatures for coupled predictions of stage II and III colorectal cancer metastasis and fluorouracil-based adjuvant chemotherapy benefit. *FASEB J.* 2019;33:151-162. **[CrossRef]**
7. Neitzel C, Demuth P, Wittmann S, Fahrer J. Targeting Altered Energy Metabolism in Colorectal Cancer: Oncogenic Reprogramming, the Central Role of the TCA Cycle and Therapeutic Opportunities. *Cancers (Basel).* 2020;12. **[CrossRef]**
8. Parks SK, Chiche J, Pouysségur J. Disrupting proton dynamics and energy metabolism for cancer therapy. *Nat Rev Cancer.* 2013;13:611-623. **[CrossRef]**
9. Altman BJ, Stine ZE, Dang CV. From Krebs to clinic: glutamine metabolism to cancer therapy. *Nat Rev Cancer.* 2016;16:619-634. **[CrossRef]**
10. Gonzalez FJ, Xie C, Jiang C. The role of hypoxia-inducible factors in metabolic diseases. *Nat Rev Endocrinol.* 2018;15:21-32. **[CrossRef]**
11. Chen LL. The expanding regulatory mechanisms and cellular functions of circular RNAs. *Nat Rev Mol Cell Biol.* 2020;21:475-490. **[CrossRef]**
12. Goodall GJ, Wickramasinghe VO. RNA in cancer. *Nat Rev Cancer.* 2021;21:22-36. **[CrossRef]**
13. Tay Y, Rinn J, Pandolfi PP. The multilayered complexity of ceRNA crosstalk and competition. *Nature.* 2014;505:344-352. **[CrossRef]**
14. Mirzaei H, Hamblin MR. Regulation of Glycolysis by Non-coding RNAs in Cancer: Switching on the Warburg Effect. *Mol Ther Oncolytics.* 2020;19:218-239. **[CrossRef]**
15. Liang G, Liu Z, Tan L, Su AN, Jiang WG, Gong C. HIF1α-associated circDENND4C Promotes Proliferation of Breast Cancer Cells in Hypoxic Environment. *Anticancer Res.* 2017;37:4337-4343. **[CrossRef]**
16. Wang S, Zhang Y, Cai Q, Ma M, Jin LY, Weng M, et al. Circular RNA FOXP1 promotes tumor progression and Warburg effect in gallbladder cancer by regulating PKLR expression. *Mol Cancer.* 2019;18:145. **[CrossRef]**
17. Li X-N, Wang Z-J, Ye C-X, Zhao B-C, Li Z-L, Yang Y. RNA sequencing reveals the expression profiles of circRNA and indicates that circDDX17 acts as a tumor suppressor in colorectal cancer. *J Exp Clin Cancer Res.* 2018;37:325. **[CrossRef]**
18. Yamamoto YH, Noda T. Autophagosome formation in relation to the endoplasmic reticulum. *J Biomed Sci.* 2020;27:97. **[CrossRef]**
19. Gonzalez CD, Alvarez S, Ropolo A, Rosenzvit C, Bagnes MF, Vaccaro MI. Autophagy, Warburg, and Warburg reverse effects in human cancer. *Biomed Res Int.* 2014;2014:926729. **[CrossRef]**
20. Qian Q, Zhou H, Chen Y, et al. VMP1 related autophagy and apoptosis in colorectal cancer cells: VMP1 regulates cell death. *Biochem Biophys Res Commun.* 2014;443:1041-1047. **[CrossRef]**
21. Ashwal-Fluss R, Meyer M, Pamudurti NR, et al. circRNA biogenesis competes with pre-mRNA splicing. *Mol Cell.* 2014;56:55-66. **[CrossRef]**
22. Kristensen LS, Andersen MS, Stagsted LVW, Ebbesen KK, Hansen TB, Kjems J. The biogenesis, biology and characterization of circular RNAs. *Nat Rev Genet.* 2019;20:675-691. **[CrossRef]**
23. Rotundo F, Cominetti D, El Bezawy R, et al. miR-1272 Exerts Tumor-Suppressive Functions in Prostate Cancer via HIP1 Suppression. *Cells.* 2020;9. **[CrossRef]**
24. Geng F, Lu GF, Luo YJ, et al. The emerging role of the MiR-1272-ADAM9-CDCP1 signaling pathway in the progression of glioma. *Aging (Albany NY).* 2020;13:894-909. **[CrossRef]**
25. Rodríguez ME, Catrinacio C, Ropolo A, Rivarola VA, Vaccaro MI. A novel HIF-1α/VMP1-autophagic pathway induces resistance to photodynamic therapy in colon cancer cells. *Photochem Photobiol Sci.* 2017;16:1631-1642. **[CrossRef]**